Electronic Supplementary Material (ESI) for ChemComm.

Supporting Information

Embedding magnetic nanoparticles into coordination polymers to mimic zinc ion transporter for targeted tumor therapy

Enguo Ju, Zhaowei Chen,Wei Li, Kai Dong, Zhenzhen Wang, Zhen Liu, Fang Pu, Jinsong Ren, and Xiaogang Qu**

Experimental Section

Reagents and Materials: Imidazole (99%), α, α'-dichloro-p-xylene (98%) and ascorbic acid (99.99%) were purchased from Aladdin Reagent. poly(ethylene glycol) bis(3-aminopropyl) terminated (M_n ~1 500) was obtained from Sigma-Aldrich. Dulbecco's modified Eagle's medium (DMEM), trypsin and fetal bovin serum were purchased from Sangon. Other reagents and solvents were acquired from Beijing Chemicals. All chemical agents were of analytical grade and were used directly without further purification. Ultrapure water (18.2 MΩ; Millipore Co., USA) was used throughout the experiments.

Instruments: Field emission scanning electron microscope (FESEM, S4800, Hitachi) was used to determine the morphology of the as-prepared samples. Transmission electron microscopy (TEM) measurements were carried out on a JEOL JEM-2010EX transmission electron microscope with a tungsten filament at an accelerating voltage of 200 kV. Fourier transform infrared (FT-IR) analyses were carried out on a Bruker Vertex 70 FT-IR spectrometer. XPS data were obtained with an ESCALab220i-XL electron spectrometer from VG Scientific using 300 W AlKα radiations. The magnetization of the nanoparticles was investigated magnetometer (Quantum Design, MPMS XL-7) at 300 K. Ultraviolet-visible spectroscopy (UV-vis) measurements were recorded on a Jasco-V550 UV-vis spectrophotometer.^{1}H spectra were recorded on Bruker AV 400 NMR spectrometer. Zeta potentials were estimated on a Zeta Potential/BI-90Plus particle size analyzer (Brookhaven, USA). The crystallographic data for the structure of coordination polymer was obtained from Cambridge Crystallographic Data Center (No.CCDC-100532).

Synthesis of Ligand bix: Bix was synthesized according to the previous reported literature. Briefly, a solution containing imidazole (3.16 g, 46.4 mmol) and α, α'-dichloro-p-xylene (0.78 g, 4.46 mmol) in methanol (50 mL) was heated under reflux for 18 h. The yellow syrup after removal of methanol by evaporation was then dissolved in aqueous K_2CO_3 (6.13 g, 100 mL). After standing for some time, this solution yielded crystalline bix dehydrate, which was further recrystallized from water.

^{1}H NMR (300 MHz, $CDCl_3$) δ: 7.54 (s, ^{2}H, N=CH-N), 7.14 (s, ^{4}H, Ph-H), 7.09 (s, ^{2}H, CH=CH-N), 6.89 (s, ^{2}H, CH-N=CH_2), 5.12 (s, ^{4}H, $PhCH_2$) (Figure S1).

Synthesis of Fe_3O_4 Nanopartilces: DHAA capped Fe_3O_4 nanoparticles were prepared as follows: $FeCl_3$•$6H_2O$ (0.27 g) was dissolved in water (10 mL), which was then added into a solution of $NaHCO_3$ (0.45 M, 20 mL). The mixture was stirred for 30 min to form a $Fe(OH)_3$ colloidal solution. Subsequently, an aqueous solution of vitamin C (16.7 mM, 10 mL) was gradually added. The mixture was further stirred for another 10 min and then transferred into a steel-lined Teflon autoclave. The autoclave was heated to and kept at 190 ºC for 4 h and then cooled to room temperature. The black nanoparticles were washed three times with water and ethanol through repeated centrifugation and re-dispersion. Finally, the obtained precipitate was dispersed in water or ethanol by ultrasonication for further use.

Synthesis of Fe_3O_4/CPs Nanoparticles: The as prepared Fe_3O_4 (5 mg) was firstly suspended in ethanol solution (10 mL) and ultrasonicated for 10 min to obtain a well-dispersed suspension. After that, an ethanolic solution of $Zn(NO_3)_2$•$6H_2O$ (0.132 M, 6.6×3 μL) and an ethanolic solution of bix (0.202 M, 3.3×3 μL) were alternate added stepwise under ultrasound condition. The mixture were allowed to be ultrasonicated for another 10 min and then centrifuged and washed with ethanol for three times to remove the unreacted regents. The final product was placed under high vacuum to remove the remaining solvent to obtain Fe_3O_4/CPs.

Surface Modification of Fe_3O_4/CPs with PEG (PEG-Fe_3O_4/CPs): To produce the PEG coating, Fe_3O_4/CPs (5 mg) was dispersed in 10 mL H_2O under ultrasonication and then mixed with 0.5 mL poly(ethylene glycol) bis(3-aminopropyl) terminated (20 mM). After ultrasonication for 30 min, the product was centrifuged at 10 000 rpm and washed by water for three times to remove excess PEG molecules. The final PEG-modified Fe_3O_4/CPs was re-suspended in water, saline or cell culture medium by ultrasonication.

Cell Culture: Human hepatoma cells (HepG 2) were cultured with regular growth media consisting of high glucose DMEM. The cell growth media were supplemented with 10% FBS, 100 U/mL penicillin, and 100 mg/mL streptomycin and cultured at 37

°C in a 5% CO_2 humidified environment. The media was changed every three days and the cells were digested by trypsin and re-suspended in fresh medium before plating.

Cytotoxicity Test: HepG 2 cells were seeded at a density of 5 000 cells/well (100 μL) in 96-well plates for 24 h. Then, PEG-Fe_3O_4/CPs, at the indicated concentrations (0, 10, 20, 40, 60, 80 and 160 μg/mL), were added to the cell culture medium. Cells were incubated with the nanoparticles for 24 h. MTT assay was used to determine the cytotoxicity. Briefly, the media was removed and the cells were washed with PBS twice. Then, 10 μL of MTT solution (5 mg/mL) was added to each well to a final volume of 100 μL. After that, the plate was placed in the CO_2 incubator for additional 4 h. The media was removed and DMSO (100 μL) was added into each well. The plate was then gently swirled for 2 min at room temperature at dark to dissolve all formed precipitate. Absorbance values were determined with Bio-Rad model-680 microplate reader at 490 nm (corrected for background absorbance at 630 nm). The cell viability was estimated according to the following equation: Cell Viability (%) = $(OD_{Treated}/OD_{Control}) \times 100\%$. Where $OD_{Control}$ was obtained in the absence of nanoparticles, and $OD_{Treated}$ was obtained in the presence of nanoparticles.

Magnetic Targeting Specific Therapy *in vitro*: HepG 2 cells were seeded at a density of 10^5 cells in a plate and allowed to adhere overnight. After the culture medium was replaced by fresh DMEM containing PEG-Fe_3O_4/CPs, a cylindrical permanent magnet was positioned at the bottom center of the plate and kept for 30 min. The dispersive PEG-Fe_3O_4/CPs would be attracted and accumulated on the circle edge of the magnet. After the removal of the magnet and the cells were incubated at 37 ºC in 5% CO_2 for another 12 h, the cells were washed mildly with PBS twice. Afterwards, the treated cells were co-stained with Calcein AM and propidium iodide (PI) for 15 min, washed with PBS, and then imaged using an Olympus BX-51 optical system microscope.

Cellular Uptake and Location: HepG 2 cells were seeded in 24-well plates and allowed to adhere overnight, then the FITC encapsulated PEG-Fe_3O_4/CPs at various concentrations were introduced into the plates containing the cells. After incubation

for 4 h, the cells were washed with PBS twice and then 500 μL fixing solution (1% glutaradehyde and 10% formaldehyde) was added to each well for 30 min. Fluorescence imaging was performed with an Olympus BX-51 optical equipped with a CCD camera to monitor the cellular uptake of the nanoparticles. The Lysosome imaging was performed with the aid of LysoTracker Red probe. Briefly, after the cells incubation with PEG-Fe_3O_4/CPs for indicated time (0.5 h, 1 h, 2 h, and 4 h), the cells were washed twice with PBS and treated with LysoTracker Red for 30 min for lysosome staining.

Determination of Cellular Concentration of Zinc: The intracellular Zn^{2+} was monitored by a zinc sensitive fluorescent probe, zinquin ethyl ester. HepG 2 cells were seeded in 24-well plates for 24 h and then incubated with PEG-Fe_3O_4/CPs (0, 10 μg/mL, 20 μg/mL, and 40 μg/mL) for 4 h. Then, the cells were washed with PBS twice and loaded with 25 μM of the Zn^{2+} probe for 10 min. Subsequently, the cells were rinsed twice with PBS and then observed using a fluorescence microscope.

Cell Apoptosis Analysis: The apoptosis of the cells were detected using the Annexin V-FITC Apoptosis detection Kit (BestBio). Briefly, HepG 2 cells were seed in 6-well plates with a density of 10^5 cells for 24 h. After treated with PEG-Fe_3O_4/CPs for 24 h, cells were collected by trypsinization and washed twice with PBS and re-suspended in Annexin V binding buffer. Further incubation was performed in Annexin V and PI at room temperature for 15 min in the dark, and then cells were subjected to flow cytometry analysis (BD LSRFortessa).

Determination of ROS Generation: HepG 2 cells were firstly seeded in 6-well plates in DMEM for 24 h before further manipulation. Then cells were treated with different concentrations of PEG-Fe_3O_4/CPs for 12 h. The treated cells were incubated with 10 μM of the fluorescent probe DCFH-DA and monitored by flow cytometry (excitation at 488 nm, emission at 530 nm).

Animal Experiments: Animal care and handing procedures were according to the guidelines of the Regional Ethics Committee for Animal Experiments. Healthy female Kunming mice (4~5 weeks) were purchased from the Laboratory Animal Center of Jilin University (Changchun, China).

Tumor Models: Hepatoma 22 (H22) tumor bearing mice were chose as the animal model to assess the antitumor effect. The cell lines were passaged 3-5 days through the mice weighing about 30 g in the form of ascites. H22 cells were harvested from the peritonea cavity of mice 7~9 days after inoculation. Then, the cells were suspended in saline at a concentration of 2×10^6 cells/mL, and 0.1 mL aliquots were subcutaneously inoculated into the oxter region of mice. Tumors were allowed to grow to ~50 mm^3 before experiment.

Biodistribution: Biodistribution was evaluated in tumor-bearing female mice. 150 μL of PEG-Fe_3O_4/CPs (5 mg/mL) in physiological saline were injected via the tail vein in each mouse (n=3). Analysis was performed by measuring the Fe content in different tissues 24 h after injection. Examined tissues include heart, liver, spleen, lung, kidneys, and tumor. Organs and tumors were washed with PBS buffer and lyophilized for 1 day. The dried tissues were mashed and dissolved in aqua regia (2 mL for liver and 1 mL for all others) for 1 day. Tissue debris was removed by centrifugation at 10 000 rpm for 5 min. After dilution, the Fe content was detected by inductively coupled plasma mass spectrometry (ICP-MS).

Anticancer effect in tumor-xenografted mice: Tumor bearing mice were randomly allocated to four groups (n=4 mice/group) for different formulations. For intratumorally injection, 50 μL of PEG-Fe_3O_4/CPs saline solution (3 mg/mL) was injected directly into the tumor. For intravenous injection, 150 μL of saline or Fe_3O_4 (5 mg/mL) or PEG-Fe_3O_4/CPs (5 mg/mL) were injected via the tail vein and then a button magnet was temporarily fixed on the tumor for 1 h. The tumor dimensions (length and width) were measured using a caliper every other day after the treatment. The tumor volume was calculated as length × $width^2/2$ (mm^3). The relative tumor volume was normalized to its initial size before administration. The mice were sacrificed after 2 weeks, and the tumors were collected and taken photos.

Histology: For histology, major organs and tumor were harvested from mice 24 h after injection. Organs were fixed in neutral buffered formalin, processed routinely into paraffin, sectioned into ~4 μm, and stained with hematoxylin and eosin (H&E). The histology was performed in college of Basic Medical Sciences of Jilin University.

The samples were examined by an Olympus BX-51 microscope in bright field.

Statistical Analysis: All the experiments were repeated at least three times, and the data are represented as means ± standard deviation (SD). The statistical analysis was performed by using Origin 8.0 software.

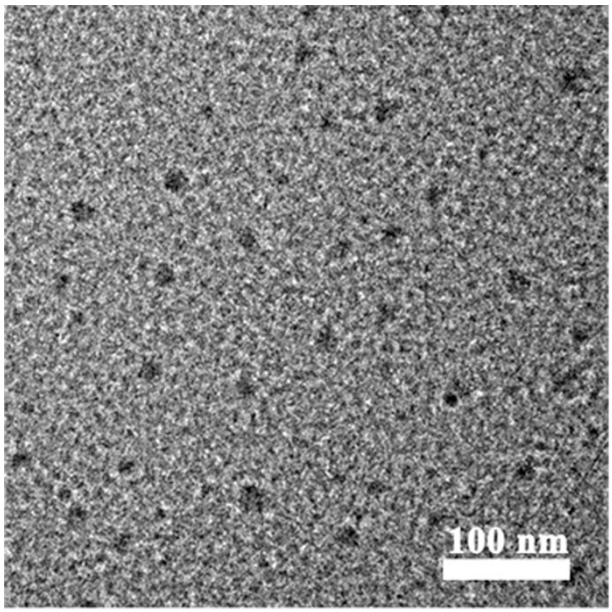

Figure S1. TEM image of DHAA-capped Fe_3O_4 nanoparticles.

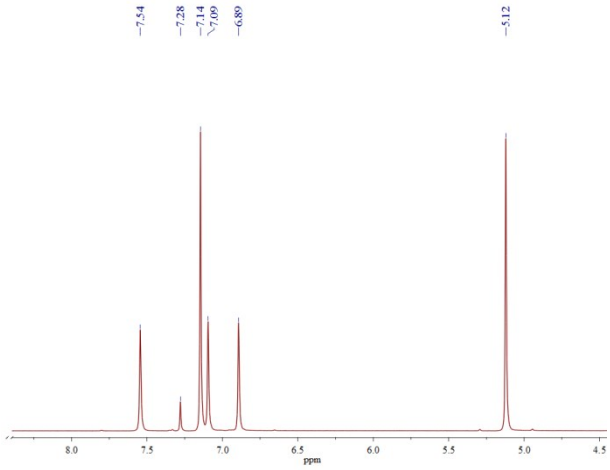

Figure S2. ^1H NMR (300 MHz, $CDCl_3$) spectra of the synthesized bix.

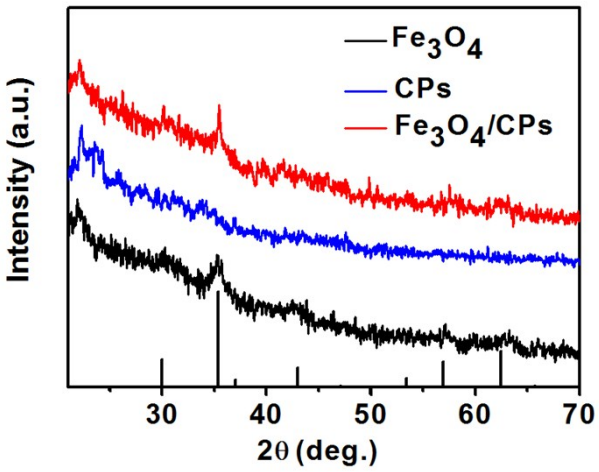

Figure S3. XRD pattern of Fe_3O_4 nanoparticles, CPs, and Fe_3O_4/CPs. It revealed that the Fe_3O_4/CPs nanocomposites were formed by cubic Fe_3O_4 (JCPDS No. 65-3107) and amorphous structure of CPs.

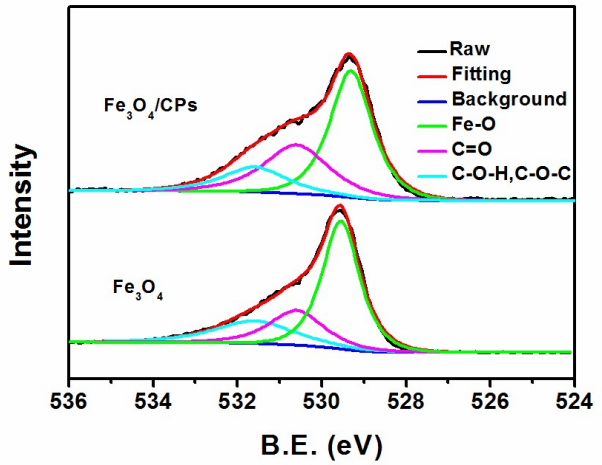

Sample	O1s (Fe-O)	O1s (C=O)	O1s (C-OH, C-O-C)
Fe_3O_4	56.21%	22.52%	21.26%
Fe_3O_4/CPs	52.87%	31.17%	15.95%

Figure S4. High-resolution XPS of O 1s revealed that peak of O 1s could deconvolute into three peaks, which are associated with oxygen in hydroxyl or ethers, oxygen in carbonyl groups, and oxygen atoms bound to metal Fe atoms. It should be mentioned that the ratio of oxygen in hydroxyl or ethers in Fe_3O_4 decreased from 21.26% to 15.95% in Fe_3O_4/CPs, which was an indirectly evidence of the coordination of Zn^{2+} with the oxygen in hydroxyl of DHAA-capped Fe_3O_4

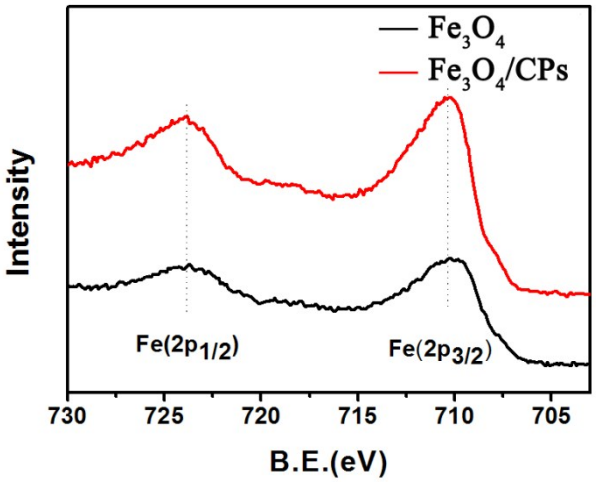

Figure S5. X-ray photoelectron spectra showing the Fe 2p level in Fe_3O_4 and Fe_3O_4/CPs nanoparticles.

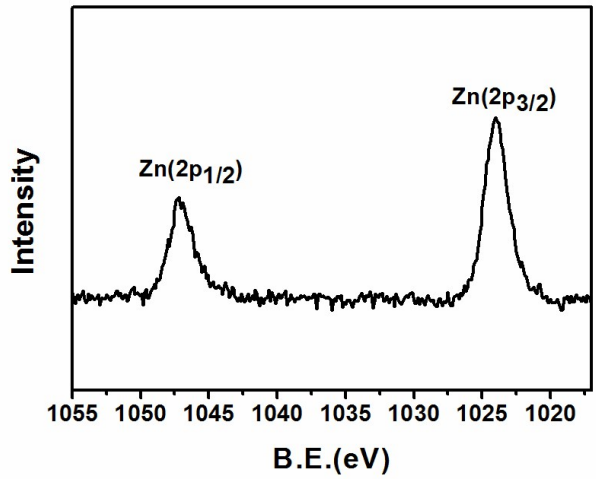

Figure S6. X-ray photoelectron spectra of Zn 2p in the Fe_3O_4/CPs nanocomposites.

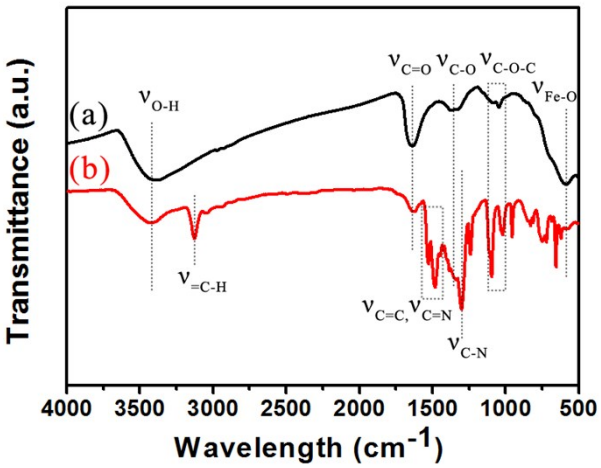

Figure S7. Fourier transform infrared (FT-IR) spectra of the (a) Fe_3O_4 and (b) Fe_3O_4/CPs nanoparticles. For Fe_3O_4 nanoparticles, the bands at 590, 1049, 1105, 1362, 1644, and 3391 cm^{-1} were attributed to Fe-O vibrations, the C-O-C and C-O stretches of the lactone ring, the C=O stretches of the carbonyl group coordinated to the Fe center and O-H stretches. As for Fe_3O_4/CPs nanocomposites, the new bands at 3135, 1529, 1490 and 1238 cm^{-1} were assigned to the aromatic C-H stretches, aromatic C=C stretches, C=N vibration and C-N vibration, which confirmed the coordination of bridging zinc ions to the bix ligands and DHAA-capped Fe_3O_4. The exposed hydroxyl groups may provide a hydrophilic component to increase the water solubility of Fe_3O_4/CPs.

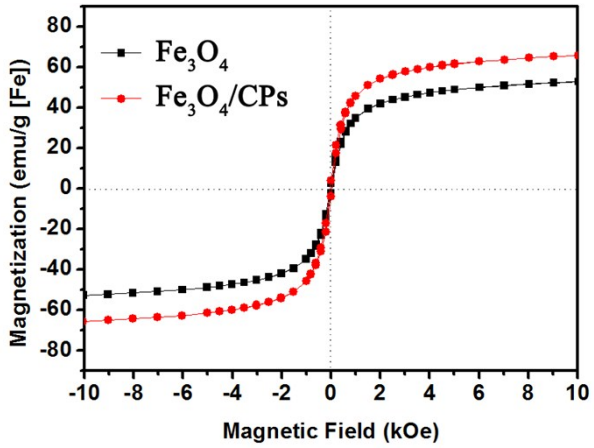

Figure S8. Hysteresis loop of the Fe_3O_4 and Fe_3O_4/CPs nanoparticles.

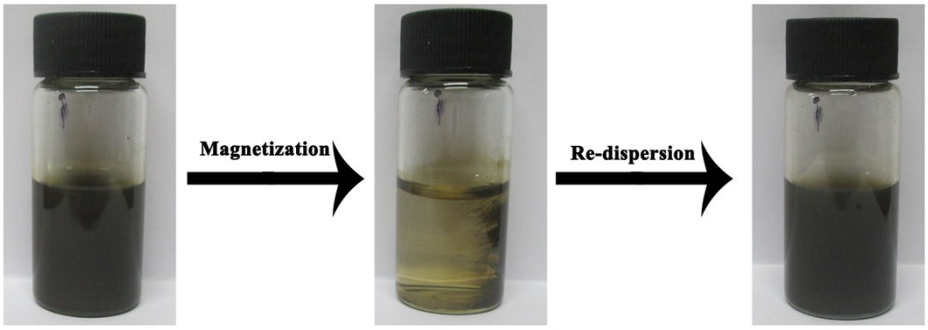

Figure S9. Photos of the magnetic aggregation and re-dispersion process of Fe_3O_4/CPs.

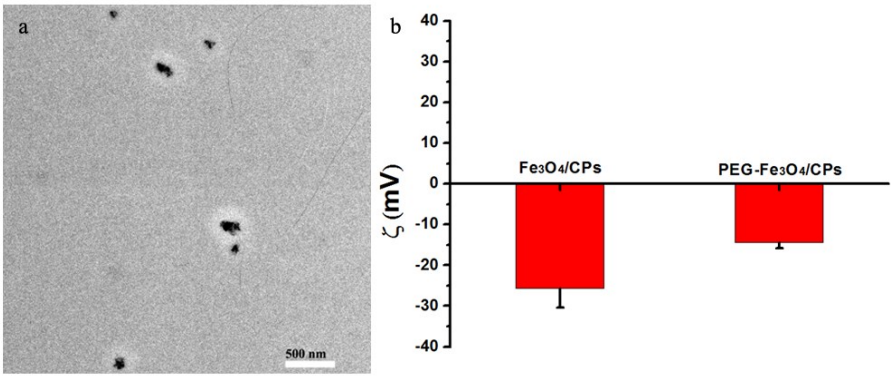

Figure S10. (a) TEM image of PEG-Fe_3O_4/CPs. (b) Zeta potential of Fe_3O_4/CPs and PEG-Fe_3O_4/CPs.

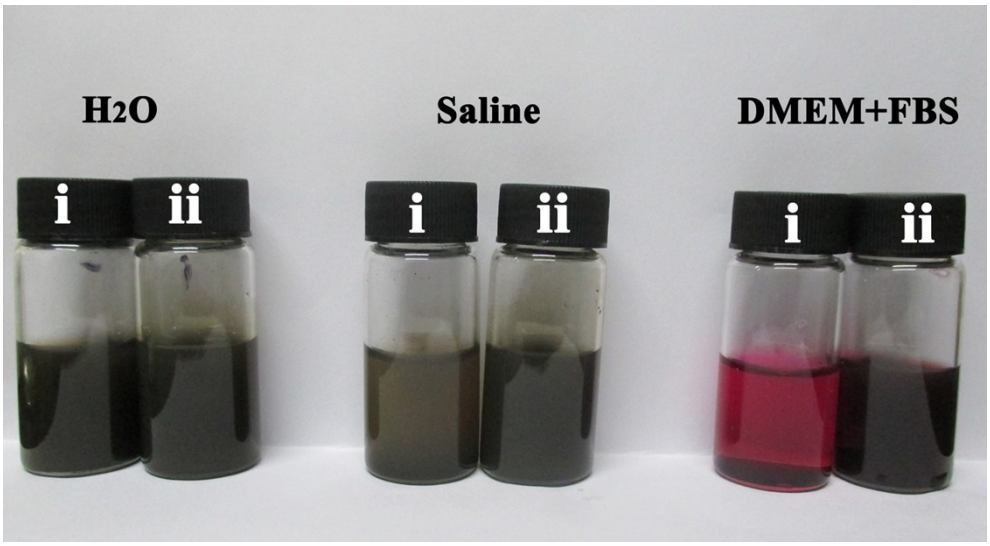

Figure S11. Photographs of Fe_3O_4/CPs (i) and PEG-modified Fe_3O_4/CPs (ii) dispersed in water, PBS, and DMEM medium with 10% FBS for 4 h.

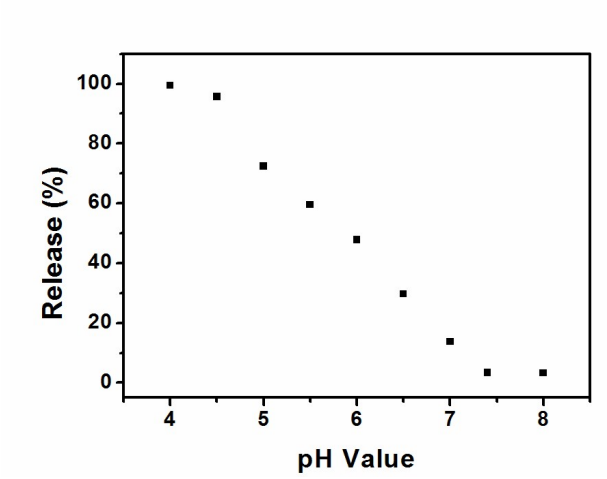

Figure S12. The release plots at different pH values.

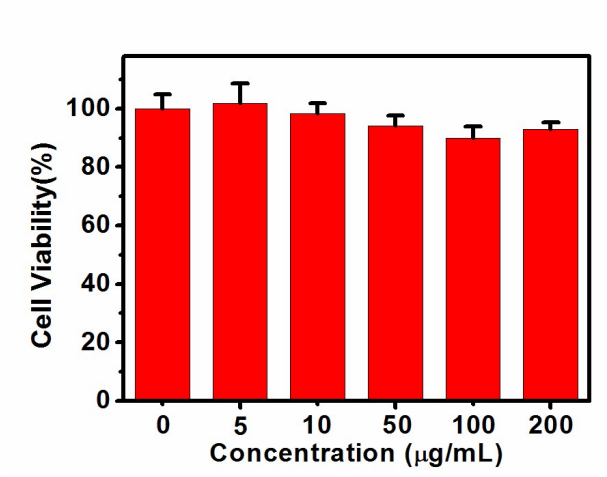

Figure S13. Cell viability of Fe_3O_4 nanoparticles.

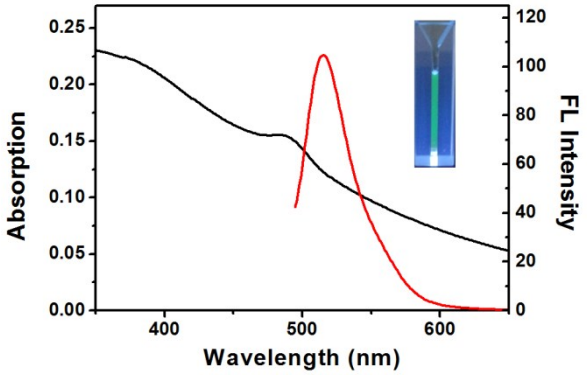

Figure S14. UV/Vis absorption spectra and fluorescence spectra of FITC-encapsulated PEG-Fe_3O_4/CPs.

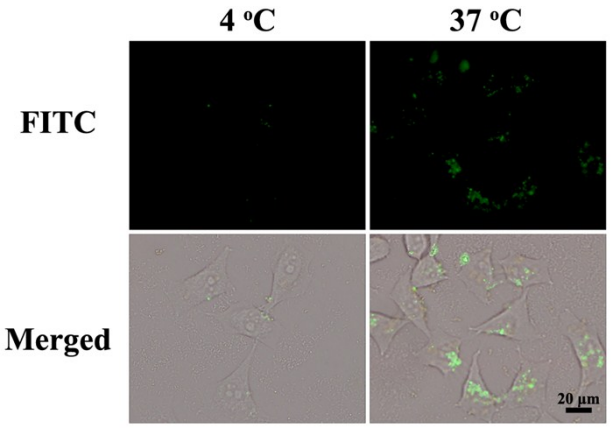

Figure S15. Cell uptake of FITC-encapsulated PEG-Fe_3O_4/CPs (20μg mL^{-1}) at 4 ºC and 37 ºC. The uptake of nanoparticles was neglectable at 4 ºC, indicating that PEG-Fe_3O_4/CPs entered cells via endocytosis, which was suppressed at 4 ºC.

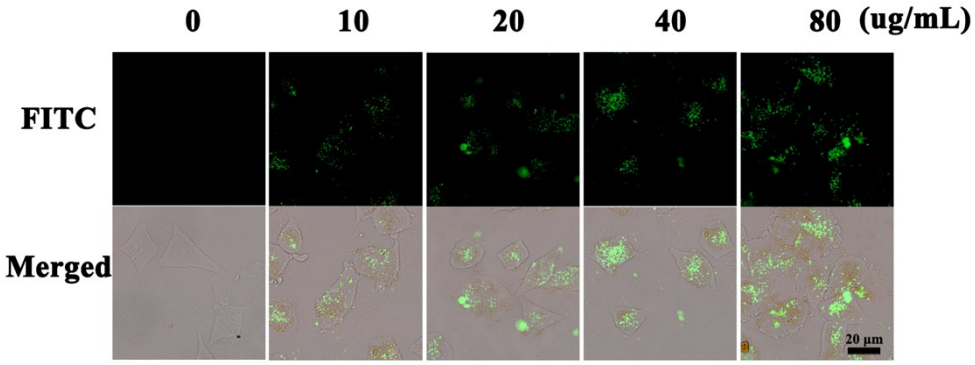

Figure S16. Cell uptake of various concentrations of FITC-encapsulated PEG-Fe_3O_4/CPs. Cells were incubated with nanoparticles for 4 h at 37 ºC and then observed under fluorescence microscope.

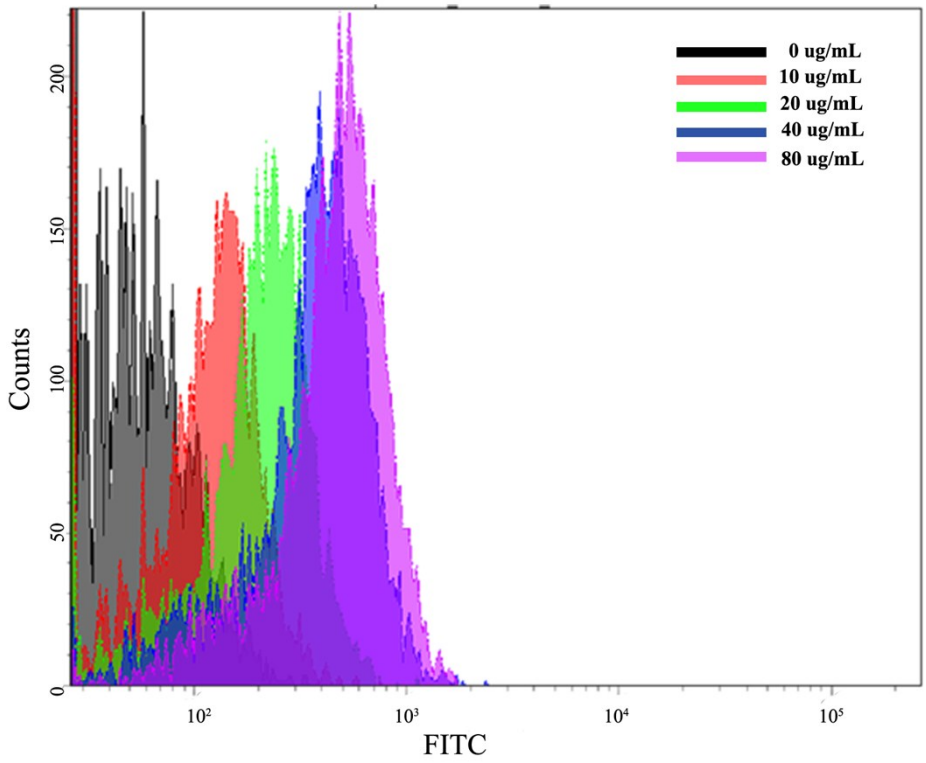

Figure S17. Quantitative analysis of cell uptake of FITC-encapsulated PEG-Fe_3O_4/CPs by flow cytometry.

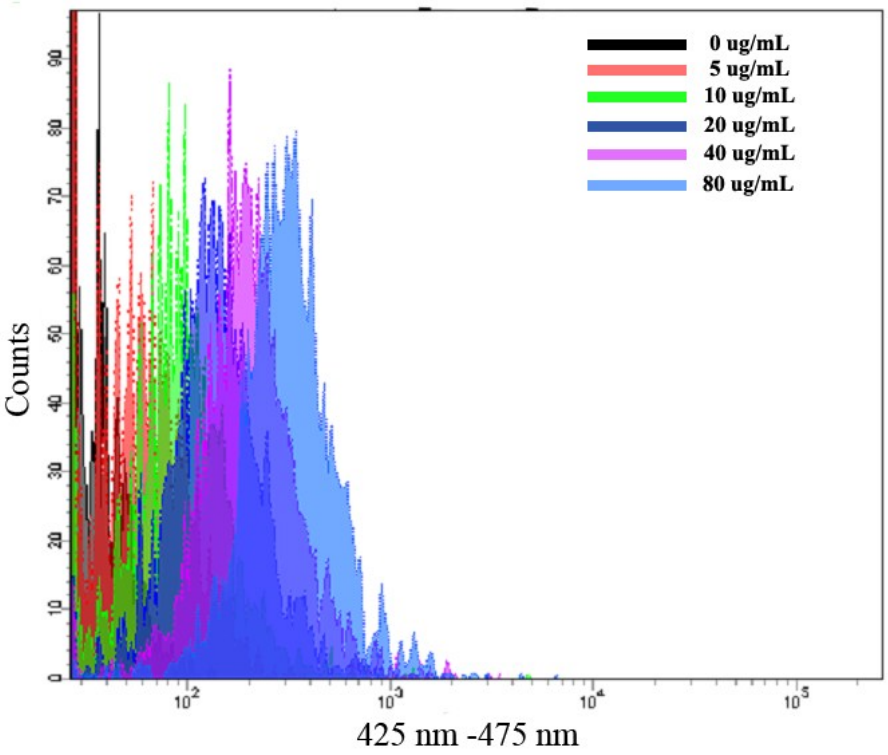

Figure S18. Flow cytometry of cells incubated with different concentrations of PEG-Fe_3O_4/CPs and then stained with a Zn^{2+} probe.

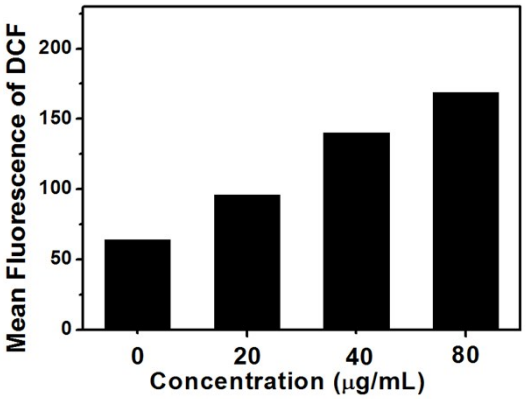

Figure S19. The mean fluorescence of DCF recorded by flow cytometry was used to monitor the production of ROS.

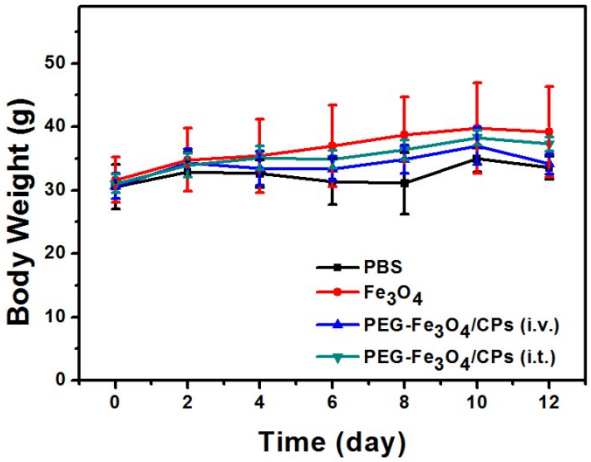

Figure S20. Time-dependent body weight of mice treated with different treatment, showing no significant change in body weight.

Figure S21. Photographs of the major organs from mice 15 days after intravenously injection of PEG-Fe_3O_4/CPs.

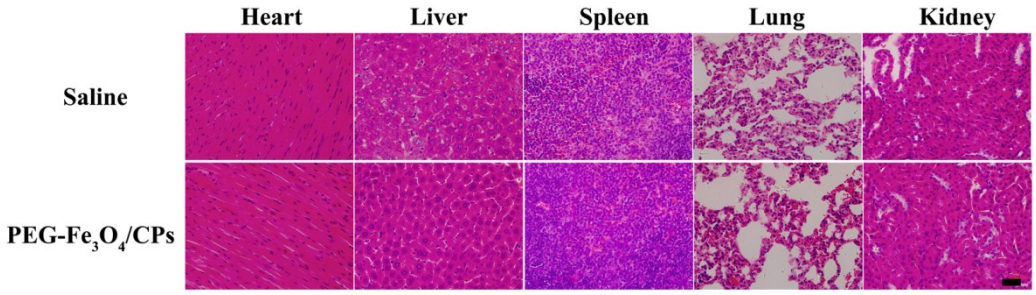

Figure S22. Representative H&E stained images of major organs including heart, liver, spleen, lung, and kidney collected from mice 15 days after intravenously injection of PBS and PEG-Fe_3O_4/CPs (scale bar = 20 μm).

Table S1| Biodistribution of PEG-Fe_3O_4/CPs at 4 h after i.v. injection. These results show mean of iron contents in these organs, n=3. (μg g^{-1})

Magnet	Heart	Liver	Spleen	Lungs	Kidneys	Tumor
+	67.06	199.05	114.89	38.70	24.69	100.39
-	80.31	190.33	186.57	49.35	32.75	44.43